Crystal Structure of Ribonuclease T1 Carboxymethylated at Glu58 in Complex with 2′-GMP‡

Kohki Ishikawa§ and Ei-ichiro Suzuki*

Central Research Laboratories, Ajinomoto Company, Inc., Suzuki-cho, Kawasaki-ku, Kawasaki 210, Japan

Masaru Tanokura

Biotechnology Research Center, University of Tokyo, Yayoi, Bunkyo-ku, Tokyo 113, Japan

Kenji Takahashi

Tokyo University of Pharmacy and Life Science, Horinouchi, Hachioji, Tokyo 192-03, Japan

Received February 28, 1996; Revised Manuscript Received April 26, 1996⊗

ABSTRACT: The carboxymethylation of RNase T1 at the γ-carboxyl group of Glu58 leads to a complete loss of the enzymatic activity while it retains substrate-binding ability. Accompanying the carboxymethylation, RNase T1 undergoes a remarkable thermal stabilization of 9 °C in the melting temperature (T_m). In order to clarify the inactivation and stabilization mechanisms of RNase T1 by carboxymethylation, the crystal structure of carboxymethylated RNase T1 (CM-RNase T1) complexed with 2′-GMP was determined at 1.8 Å resolution. The structure, including 79 water molecules and two Na^+, was refined to an *R* factor of 0.194 with 10 354 reflections $>1\sigma(F)$. The carboxyl group of CM-Glu58, which locates in the active site, occupies almost the same position as the phosphate group of 2′-GMP in the crystal structure of intact RNase T1·2′-GMP complex. Therefore, the phosphate group of 2′-GMP cannot locate in the active site but protrudes toward the solvent. This forces 2′-GMP to adopt an *anti* form, which contrasts with the *syn* form in the crystal of the intact RNase T1·2′-GMP complex. The inaccessibility of the phosphate group to the active site can account for the lack of the enzymatic activity in CM-RNase T1. One of the carboxyl oxygen atoms of CM-Glu58 forms two hydrogen bonds with the side-chains of Tyr38 and His40. These hydrogen bonds are considered to mainly contribute to the higher thermal stability of CM-RNase T1. Another carboxyl oxygen atoms of CM-Glu58 is situated nearby His40 and Arg77. This may provide additional electrostatic stabilization.

Ribonuclease T1 (RNase T1;[1] EC 3.1.27.3) from the fungus *Aspergillus oryzae* is an enzyme that specifically hydrolyzes a phosphate diester bond at the 3′-side of guanosine in single-stranded RNA (Sato & Egami, 1957). RNase T1 is a globular protein with 104 amino acid residues (M_r 11 085) in a single polypeptide chain (Takahashi, 1965). Since RNase T1 is a small, stable enzyme, a number of studies, including chemical modifications (Takahashi & Moore, 1982), protein engineering (Nishikawa et al., 1987; Steyaert et al., 1990, etc.), NMR (Inagaki et al., 1981, etc.), and X-ray crystallography (Heinemann & Saenger, 1982, etc.), have been performed on this protein. These studies have elucidated that His40, Glu58, Arg77, and His92 are involved in the active site. As regards the crystallographic studies, many crystal structures, the free form (Martinez-Oyanedel et al., 1991), and the complexed forms with 2′-guanylic acid (2′-GMP; Arni et al., 1987; Sugio et al., 1988), 3′-guanylic acid (3′-GMP; Heydenreich et al., 1993; Gohda et al., 1994), guanylyl-2′,5′-guanosine (2′,5′-GpG; Koepke et al., 1989), guanosine-3′,5′-bisphosphate (3′,5′-pGp; Lenz et al., 1993), and vanadate ($H_2VO_4^-$; Kostrewa et al., 1989), have been determined. These crystal structures have played especially important roles in elucidating the enzymatic mechanism and the nucleotide binding modes. Furthermore, some mutant proteins of RNase T1 have been subjected to crystallographic studies to allow more detailed discussions on this enzyme [for example, Tyr45Trp complexed with 2′-AMP and 2′-GMP (Hakoshima et al., 1992)].

Takahashi et al. (1967) reported that RNase T1 is completely inactivated by the selective carboxymethylation of the γ-carboxyl group of Glu58 (-COO^- → -COOCH2COO^-) with iodoacetate at pH 5.5. The Glu58 carboxylate has been proposed to act as base in a general acid−base catalysis (Takahashi, 1970a; Heydenreich et al., 1993). Despite the loss of the enzymatic activity, carboxymethylated RNase T1 (CM-RNase T1) retains almost the same binding ability against guanosine and 10% binding ability against 2′-GMP as compared to intact RNase T1, in terms of the K_d values (Takahashi & Moore, 1982). This suggested that the carboxymethylation of Glu58 affects only the binding of phosphate portion and hardly affects that of guanosine.

To compare the thermal stability of CM-RNase T1 with that of intact RNase T1, ^{1}H NMR spectra measurement was performed at various temperatures and the changes in the peak areas were plotted for two specific protons (Kojima et al., 1994). It turned out that the T_m value of CM-RNase T1 is higher than that of intact RNase T1 by 9 °C ($\Delta\Delta G$ = 5.25 kcal/mol). Kojima et al. (1994) ascribed this remarkable

‡ The atomic coordinates and structure factors have been deposited with the Protein Data Bank (ID Code 1DET).

* To whom correspondence should be addressed.

§ University of Tokyo.

⊗ Abstract published in *Advance ACS Abstracts,* June 1, 1996.

[1] Abbreviations: CM-RNase T1; ribonuclease T1 carboxymethylated at the γ-carboxyl group of Glu58; 2′-GMP; 2′-guanylic acid; T_m, melting temperature.

S0006-2960(96)00493-X CCC: $12.00

stabilization effect to the formation of a strong salt bridge between CM-Glu58 and its proximal residue, Arg77.

In this paper, we describe the crystal structure of CM-RNase T1 complexed with 2′-GMP determined at 1.8 Å resolution. A comparative study of the three-dimensional structures of CM-RNase T1 and intact RNase T1 allows us to elucidate the mechanism of the inactivation and thermal stabilization of RNase T1 upon carboxymethylation at Glu58.

MATERIALS AND METHODS

Crystallization. CM-RNase T1 was prepared as described previously (Takahashi et al., 1967). Crystallization was carried out using the sitting-drop vapor diffusion technique. Typically, 15 μL of the drop, containing 10 mg of protein/mL, 0.5% 2′-GMP, 30 mM sodium citrate (pH 3.2), and 17% (v/v) 2-methylpentane-2,4-diol, was equilibrated against a 51% (v/v) 2-methylpentane-2,4-diol solution at 20 °C. The final pH value of this crystallization buffer was 4.5. Cube-shaped crystals appeared and grew to around 0.6 mm within a few weeks. The crystals belonged to the space group $I23$ with unit cell parameters $a = b = c = 88.69$ Å and contained one molecule per asymmetric unit. The calculated packing density of the crystal, V_m, is 2.61 Å^3/Da, and the corresponding solvent content is 52.9% (Matthews, 1968).

Data Collection. The X-ray intensity data used in this study were collected using the macromolecule-oriented Weissenberg camera (Sakabe, 1991), installed at the Beam Line 6A of the Synchrotron Radiation Source at the National Laboratory for High Energy Physics, Tsukuba. The wavelength was set to 1.00 Å. Only one crystal was necessary to collect the whole data set. The diffraction patterns were recorded on imaging plates and were digitized by a BA-100 reader (Fuji Film). The diffraction data were processed using the program WEIS (Higashi, 1989), and scaling between imaging plates was performed using the CCP4 program suite (Collaborative Computational Project, Number 4, 1994). The merging $R(I)$ factor ($\sum_i I_i - \langle I_i \rangle / \sum_i I_i$, where $\langle I_i \rangle$ is the average of I_i over all symmetrical equivalents) for data up to 1.8 Å resolution was 0.057 for 10 459 unique reflections [$I > \sigma(I)$]. This data set was 95.9% complete to 1.8 Å resolution and 89.7% complete in the resolution shell between 1.89 Å and 1.80 Å.

Structure Determination. Since the crystal of CM-RNase T1·2′-GMP is nearly isomorphous with that of intact RNase T1·3′,5′-pGp (Lenz et al., 1993; space group; $I23$, $a = 87.06$), the crystal structure of this complex was used as a starting model. Although this crystal structure has been refined to 1.9 Å resolution, it was unfortunately not registered in the Brookhaven protein data bank (PDB). Therefore, the crystal structure refined at 3.2 Å resolution (Lenz et al., 1991; PDB code 5RNT) was used instead. Water and 3′,5′-pGp molecules were excluded from the starting model. This model was subjected to rigid-body refinement using the program package X-PLOR (Brünger et al., 1987). Reflections ranging from 10.0 to 3.0 Å were used for the calculation. The crystallographic R factor was reduced from 0.550 to 0.382.

Subsequent simulated-annealing refinement using the X-PLOR and intensity data between 10.0 and 2.3 Å yielded an R factor of 0.278. Since the calculated electron-density map clearly indicated the presence of 2′-GMP and the carboxymethyl group of CM-Glu58, they were included in the model at this stage. Furthermore, Lys25 was replaced by Gln, as the amino acid at position 25 of this enzyme used in this study is Gln, instead of Lys in its variant form which has been subjected to most of the crystallographic studies performed so far (Heinemann & Saenger, 1982, etc.). An additional round of simulated annealing resulted in an R factor of 0.247 (10.0−2.3 Å). Then, the refinement was followed using the least-squares refinement program PROLSQ (Hendrickson & Konnert, 1980), allowing the individual temperature factors to be refined. In the course of refinement, some side chains were remodeled, and solvent molecules were located on the protein surface. Val78 was shown to have two discrete conformations. The final R factor for 10 354 reflections [$F > \sigma(F)$] was 0.194 for all intensity data from 8.0 to 1.8 Å. All atoms constituting the protein and the nucleotide are clearly defined in the electron density map. The ϕ/ψ main-chain torsion angles are clustered in the allowed region of the Ramachandran plot (Ramachandran et al., 1963).

Table 1: Refinement Statistics

restraints	rms deviation[a]	target σ[b]
distances		
bond (Å)	0.019	0.020
angle (Å)	0.045	0.030
planar 1−4 (Å)	0.055	0.050
planes (Å)	0.015	0.020
chiral centers (Å^3)	0.191	0.150
nonbonded contacts		
single torsion (Å)	0.180	0.300
multiple torsion (Å)	0.196	0.300
possible h-bonds (Å)	0.234	0.300
torsion angles		
planar (deg)	2.9	3.0
staggered (deg)	17.7	15.0
orthonormal (deg)	26.0	20.0
isotropic thermal factors		
main-chain bond (Å^2)	1.424	1.000
main-chain angle (Å^2)	2.453	1.500
side-chain bond (Å^2)	2.547	1.500
side-chain angle (Å^2)	3.995	2.000

[a] The rms deviation from ideal values. [b] The target values are the input estimated standard deviations that determine the relative weights of the corresponding restraints.

The final model consists of 787 protein atoms including two additional ones for the disordered side-chain of Val78, together with 24 atoms of 2′-GMP, two Na^+, and 79 water molecules. A summary of the stereochemical parameters is presented in Table 1.

RESULTS

Overall Crystal Structure. The crystal structure of CM-RNase T1·2′-GMP was compared with that of intact RNase T1·2′-GMP refined at 1.9 Å resolution (Arni et al., 1987; PDB code 1RNT). The best superposition, which was calculated for all 104 α-carbon atoms, yielded an rms displacement of 0.49 Å. Ala1, Ser35, Gly71, Asn97, and Asn98 showed deviations larger than 1.0 Å. These residues are, however, located either at the loose N-terminus or in the loops influenced by direct intermolecular interactions in the present cubic crystal. Therefore, it can be concluded that carboxymethylation of the γ-carboxyl group of Glu58 does not affect the overall structure of RNase T1.

Catalytic Site. Figure 1 shows the structures of catalytically important residues (Tyr38, His40, Glu58, Arg77, His92) and bound 2′-GMP in the present CM-RNase T1·2′-GMP,

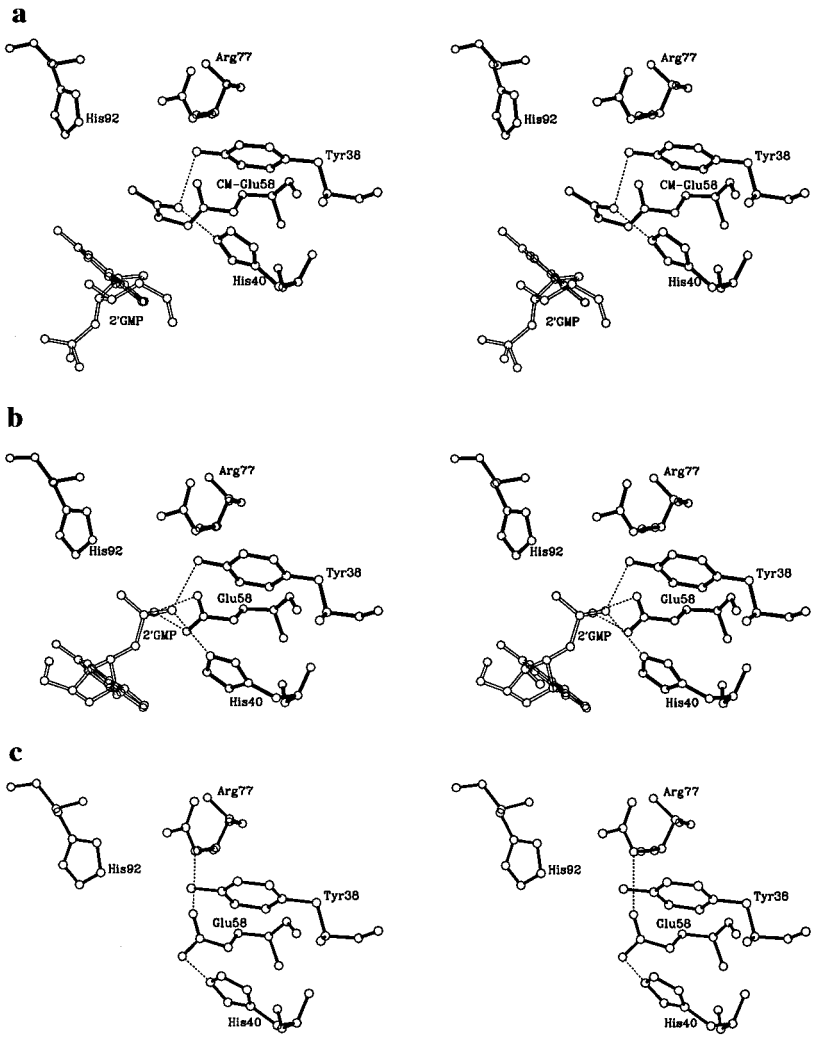

FIGURE 1: Comparison of the active-site geometry in (a) CM-RNase T1·2′-GMP (dashed lines represent the hydrogen bonds involving the carboxyl group of CM-Glu58), (b) intact RNase T1·2′-GMP (Arni et al., 1987; dashed lines represent the hydrogen bonds involving the phosphate of 2′-GMP), and (c) free intact RNase T1 (Martinez-Oyanedel, 1991; dashed lines represent the hydrogen bonds involving the carboxyl group of Glu58).

intact RNase T1·2′-GMP (Arni et al., 1987), and free intact RNase T1 (Martinez-Oyanedel, 1991).

A structural comparison of CM-RNase T1·2′-GMP with intact RNase T1·2′-GMP reveals that the position that the phosphate group of 2′-GMP takes in intact RNase T1·2′-GMP is occupied by the carboxyl group of CM-Glu58 in CM-RNase T1·2′-GMP. The carboxyl group of CM-Glu58 is fixed by two hydrogen bonds from one of its carboxyl oxygen atoms (Oθ2) to Oη of Tyr38 and Nϵ2 of His40. The distances of the hydrogen bonds are 3.1 and 2.4 Å, respectively. The presence of the carboxyl group of CM-Glu58 does not allow the phosphate group of 2′-GMP to enter the catalytic site and forces it to stay away from the binding pocket. Consequently, 2′-GMP adopts an *anti* form in contrast to the *syn* form observed in the previously reported structures of intact RNase T1 complexed with nucleotides, such as RNase T1·2′-GMP.

The conformation of CM-Glu58 is essentially the same as that of Glu58 in intact RNase T1·2′-GMP and free intact RNase T1, except for the extension of the side chain by the carboxymethylation. Tyr38 and Arg77 also show no structural differences among the structures shown in Figure 1. A salt bridge between the introduced carboxymethyl group of CM-Glu58 and the guanidino group of Arg77, which was suggested to be formed from NMR spectroscopy data (Inagaki et al., 1981), is not observed in the present crystal structure.

The position of the imidazole ring of His40 in CM-RNase T1·2′-GMP deviates by 1.59 Å from that in intact RNase T1·2′-GMP. Besides, the imidazole ring is rotated by 180°. This deviation is ascribed to the difference in the hydrogen-bonding partner of Nϵ2 in the imidazole ring. The partner is the carboxyl oxygen atom of CM-Glu58 in CM-RNase T1·2′-GMP, while it is the phosphate oxygen atom of 2′-GMP in intact RNase T1·2′-GMP. The structure of the imidazole ring in CM-RNase T1·2′-GMP is almost the same as that in free intact RNase T1.

The imidazole ring of His92 in CM-RNase T1·2′-GMP deviates by 0.81 Å when compared with that in intact RNase T1·2′-GMP, and by 1.51 Å when compared with that in free intact RNase T1. However, this imidazole ring is situated close to a symmetry-related molecule in the crystal of CM-RNase T1·2′-GMP. Therefore, this deviation can be ascribed to the intermolecular interactions and not to the carboxymethylation at Glu58.

Nucleotide Binding. The guanine base of 2′-GMP binds to CM-RNase T1 in the specific nucleotide binding site in the same manner as it binds to intact RNase T1 (Figure 2). All the hydrogen bonds that define the guanine specificity

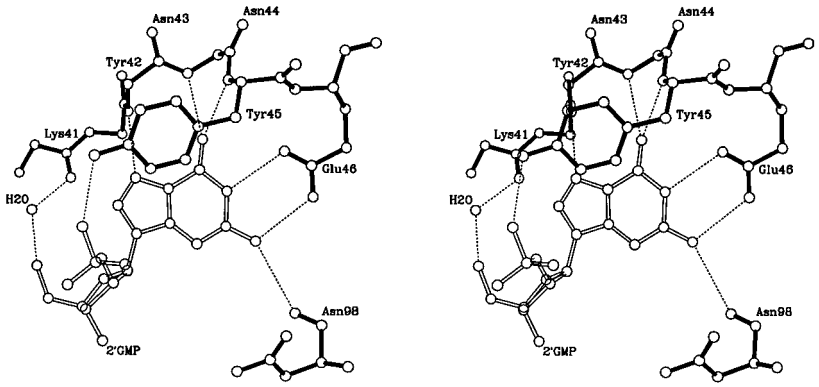

FIGURE 2: Stereoview of 2′-GMP bound to the specific nucleotide binding site in CM-RNase T1·2′-GMP.

Table 2: Hydrogen-Bonding Interactions Involving 2′-GMP[a]

group	atom	CM-RNase T1·2′-GMP		intact RNase T1·2′-GMP	
guanine	N1	Glu46 Oϵ1	2.8	Glu46 Oϵ1	2.7
	N2	Glu46 Oϵ2	2.8	Glu46 Oϵ2	3.0
		Asn98 O	3.2	Asn98 O	2.9
	O6	Asn44 N	2.8	Asn44 N	2.8
		Tyr45 N	3.0	Tyr45 N	2.8
	N7	Asn43 N	2.9	Asn43 N	3.3
ribose	O3′	2′GMP O2P (s)	3.3		
phosphate	O1P	Asn98 Nδ2 (s)	2.9	His40 Nϵ2	2.8
				Tyr38 Oη	2.7
	O2P	2′GMP O3′ (s)	3.3		
	O3P	Tyr45 Oη	2.8	Glu58 Oϵ1	2.7
				Glu58 Oϵ2	2.4

[a] (s): Symmetry-related atom. Interactions with water molecules are not listed.

of RNase T1 (Heinemann & Saenger, 1982) are completely conserved.

One of the three oxygen atoms of the phosphate group of 2′-GMP forms a single hydrogen bond with Oη of Tyr45, while the other two oxygen atoms are involved in the interactions with symmetry-related molecules in the crystal and therefore do not interact with CM-RNase T1 in solution. This contrasts to intact RNase T1·2′-GMP where the phosphate group forms four hydrogen bonds in the catalytic site (Arni et al., 1987).

A comparison of the hydrogen bonds involving 2′-GMP between CM-RNase T1·2′-GMP and intact RNase T1·2′-GMP is shown in Table 2.

Disorder of Val78. The side chain of Val78 is found in two conformations, although it is located in a hydrophobic core. This disorder of Val78 is also observed in other RNase T1 structures, such as free intact RNase T1, intact RNase T1·vanadate, and intact RNase T1·3′,5′-pGp. A common feature for these structures is that the phosphate binding site is empty. On the other hand, Val78 is ordered when a phosphate group is present in the catalytic site [for example, in the crystal structure of intact RNase T1·2′-GMP (Arni et al., 1987)]. Lenz et al. (1993) suggested that presence of a phosphate group in the catalytic site is associated with ordering of Val78. The disorder of Val78 in the present structure seems to support their proposal.

Na^+ Binding Site. Two spherical-shaped peaks in the electron density map were identified as sodium ions, which were named Na106 and Na107, respectively. One water molecule that should be coordinated to Na106 is not observed in the electron density map, probably because of a high fluctuation. Except for this, however, both sodium ions show 6-fold coordination in a nearly perfect octahedron, as shown in Figure 3. The average ligand distances for Na106 and Na107 are 2.44 and 2.52 Å, respectively.

Na106 is coordinated to the backbone carbonyl oxygen atoms of His92 and Ala95, along with two water molecules and the backbone carbonyl oxygen of Gly30 in a symmetry-related molecule. The same Na^+ binding site is also observed in the crystal structure of Glu58Ala RNase T1·2′-GMP (Pletinckx et al., 1994). A similar sodium site of Na107 has not been found in any of other RNase T1 structures.

Crystal Packing. Except for intact RNase T1·3′,5′-pGp, RNase T1 has been crystallized in space group $P2_12_12_1$ [for example, complexed form with 2′-GMP (Arni et al., 1987)] or $P2_1$ [for example, complexed form with 3′-GMP (Heydenreich et al., 1993)]. In the crystals of CM-RNase T1·2′-GMP and intact RNase T1·3′,5′-pGp that both crystallize in space group *I*23, the bound nucleotides adopt an *anti* form, compared with the *syn* form in any other crystal containing RNase T1. Therefore, it can be assumed for RNase T1 that crystallizing in space group *I*23 is associated with the *anti* form of a bound nucleotide.

The intermolecular interactions are summarized in Table 3. Residues in the catalytic site do not form any intermolecular hydrogen bond, while 2′-GMP is involved in the hydrogen bonding network with neighboring molecules.

DISCUSSION

Mechanism of Inactivation. CM-RNase T1 does not possess enzymatic activity at all (Takahashi et al., 1967). Considering the fact that mutant enzymes, Glu58Asp, Glu58Ala, and Glu58Gln, retain distinct activity (Nishikawa et al., 1987), the complete inactivation by the carboxymethylation is striking. Glu58 is no doubt an important residue for the enzymatic activity but is not always essential. In the crystal structure of intact RNase T1·3′-GMP, both His40 and Glu58 hydrogen bond to O2′ of 3′-GMP (Heydenreich et al., 1993; Gohda et al., 1994). Therefore, it is likely that His40 acts as the catalytic base in the absence of Glu58. However, the addition of a single carboxymethyl group to Glu58 deprives RNase T1 of the whole enzymatic activity.

A structural comparison of CM-RNase T1·2′-GMP with intact RNase T1·2′-GMP (Arni et al., 1987) elucidates the inactivation mechanism. The presence of the carboxymethyl group in the catalytic site prevents phosphate of nucleotide from coming into the phosphate binding site observed in the crystal structure of intact RNase T1·2′-GMP (Figure 1). The

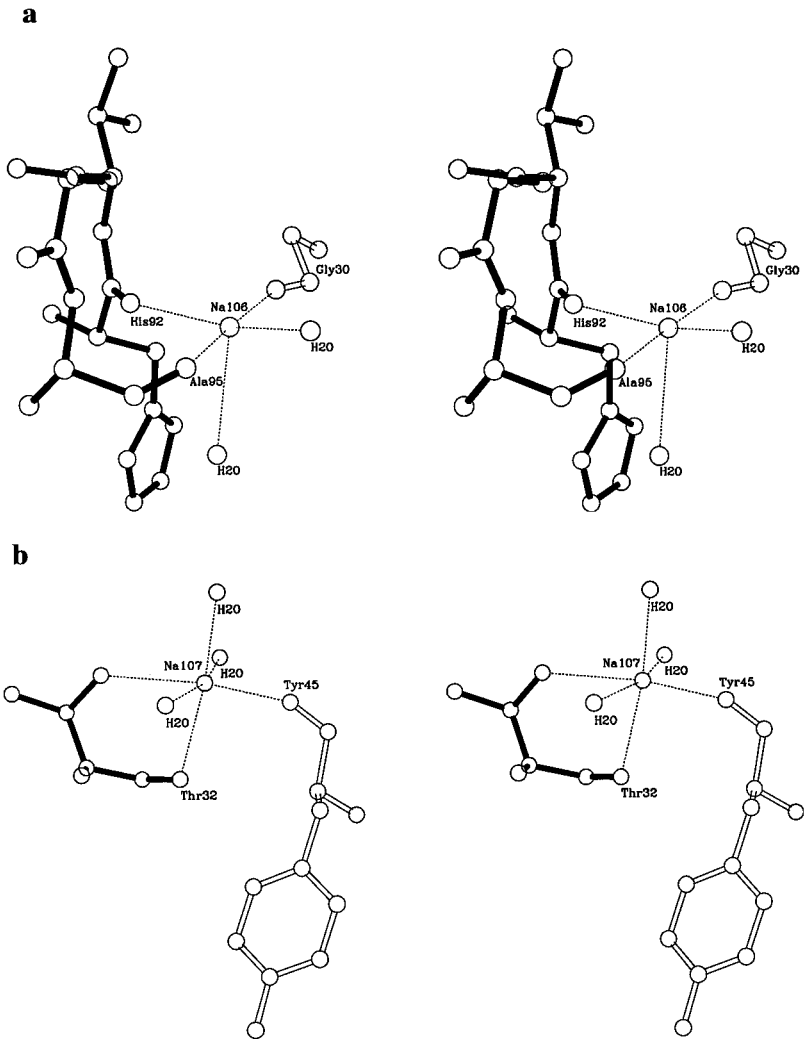

FIGURE 3: Stereoviews of Na^+ binding sites, (a) Na106, and (b) Na107 in CM-RNase T1·2′-GMP. Open bonds represent atoms in symmetry-related molecules.

Table 3: Intermolecular Ionic Interaction (≤3.5 Å)

residue	atom	residue	atom	distance (Å)	symmetry operation
Asn98	Oδ1	Asn99	Nδ2	3.0	$x,-y,z$
Asn98	Nδ2	2′-GMP	O1P	2.9	$x,-y,z$
2′-GMP	OP2	2′-GMP	O3′	3.3	$x,-y,z$
Lys41	Nζ	Ser69	Oγ	3.3	$-z+1/2,-x+1/2,y+1/2$
Asn44	Nδ2	Gly70	O	3.2	$-z+1/2,-x+1/2,y+1/2$
Ser54	Oγ	Ser69	Oγ	3.4	$-z+1/2,-x+1/2,y+1/2$
Ser54	Oγ	Gly71	N	3.2	$-z+1/2,-x+1/2,y+1/2$
Gly34	N	Asn44	O	3.0	$-y+1/2,z+1/2,-x+1/2$
Ser35	Oγ	Asp49	Oδ1	3.5	$-y+1/2,z+1/2,-x+1/2$
Glu28	O	Ala75	N	3.4	$y+1/2,-z+1/2,-x+1/2$

inaccessibility of the phosphate group to the catalytic site clearly explains the lack of enzymatic activity of CM-RNase T1.

Binding Ability Toward Nucleotide. CM-RNase T1 possesses almost the same binding ability toward guanosine as that of intact RNase T1 (Takahashi, 1972). This is quite reasonable, considering the fact that no structural difference in the specific guanine binding site is found between CM-RNase T1·2′-GMP and intact RNase T1·2′-GMP (Figure 2 and Table 2). On the other hand, the binding ability against guanylic acid is considerably lowered upon carboxymethylation at Glu58 (Takahashi & Moore, 1982). For example, the K_d values of CM-RNase T1 and intact RNase T1 against 2′-GMP are 50 and 4.8 μM, respectively, at pH 5.0 (Walz, 1977). This is explained by the difference in the number of hydrogen bonds involving phosphate of 2′-GMP. The phosphate group of 2′-GMP in CM-RNase T1·2′-GMP points toward solvent, and only one hydrogen bond (to Oη of Tyr45) is formed (Figure 2), while that in intact RNase T1·2′-GMP is situated in the catalytic site and forms four hydrogen bonds (Figure 1b).

Thermal Stabilization Upon Carboxymethylation. The T_m value of RNase T1 is increased by 9 °C ($\Delta\Delta G = 5.25$ kcal/mol) by the carboxymethylation at Glu58 (Kojima et al., 1994). The crystal structure of CM-RNase T1·2′-GMP is compared with that of free intact RNase T1 (Martinez-Oyanedel, 1991) in Figure 1a,c. Strictly speaking, the structure of free CM-RNase T1 should be used for the comparison. However, we suppose that the structure around CM-Glu58 in CM-RNase T1·2′-GMP is essentially the same as that in free CM-RNase T1, since the residues around CM-Glu58 are not involved in the interactions with either 2′-GMP or neighboring molecules in the present crystal.

In free intact RNase T1, the carboxyl group of Glu58 forms two hydrogen bonds (Figure 1c), one from Oε2 to Nε of His40 and another from Oε1 to Nε of Arg77. These hydrogen bonds are also retained in CM-RNase T1·2′-GMP.

In CM-RNase T1·2′-GMP, Oθ2 of CM-Glu58 forms two hydrogen bonds with Oη of Tyr38 and Nε2 of His40,

respectively (Figure 1a). Shirley et al. (1992) prepared 12 single mutants of RNase T1, in which up to three hydrogen bonds were removed, and proposed that an intramolecular hydrogen bond contributes 1.3 ± 0.6 kcal/mol to protein stability on the basis of urea and thermal unfolding studies of these mutants. If this value is the case, the newly formed two hydrogen bonds in CM-RNase T1 can explain half the increase in the thermal stability upon carboxymethylation.

Another oxygen atom (Oθ1) of the carboxymethyl group of CM-Glu58 is situated nearby two basic residues, Arg77 and His92 (Figure 1a). The distances from this atom to Nη2 of Arg77 and Nϵ2 of His92 are 4.2 and 4.5 Å, respectively. These are too long for those atom pairs to be called as salt bridges but are short enough to contribute to electrostatic stabilization. Since Arg77 and His92 are thought to be positively charged at pH 4.4 where the T_m values were measured (Kojima et al., 1994), the negatively charged carboxymethyl group of CM-Glu58 can play a role of reducing the surrounding positive charges. This electrostatic stabilization is probably another origin for the increased thermal stability of CM-RNase T1.

High Reactivity of Glu 58 with Iodoacetate. The hydrogen bonds involving Oθ2 of CM-Glu58 seem to indicate that the specific binding of the carboxyl group of iodoacetate to Tyr38 and His40 may serve as orienting the reagent in the carboxymethylation reaction of RNase T1. Moreover, they may stabilize the produced CM-Glu58. This explains why Glu58 is selectively carboxymethylated among the five Glu residues in RNase T1 and why the involvement of a protonated form of a His residue was indicated by the pH/rate profile of inactivation of RNase T1 with iodoacetate (Takahashi, 1970b).

ACKNOWLEDGMENT

A part of this work was performed using the Station BL6A at the Photon Factory, National Laboratory for High Energy Physics under the approval of the Photon Factory Program Advisory Committee. We are grateful to Prof. N. Sakabe for the use of the Weissenberg camera and to H. Sasaki, T. Ichikawa, and H. Koike for their assistance at the Synchrotron Radiation Source, Tsukuba.

REFERENCES

Arni, R., Heinemann, U., Maslowska, M., Tokuoka, R., & Saenger, W. (1987) *Acta Crystallogr. B43*, 548.
Brünger, A. T., Kurian, J., & Karplus, M. (1987) *Science 235*, 458.
Collaborative Computational Project, Number 4 (1994) *Acta Crystallogr. D50*, 760.
Gohda, K., Oka, K., Tomita, K., & Hakoshima, T. (1994) *J. Biol. Chem. 269*, 17531.
Hakoshima, T., Itoh, T., Tomita, K., Goda, K., Nishikawa, S., Morioka, H., Uesugi, S., Ohtsuka, E., & Ikehara, M. (1992) *J. Mol. Biol. 223*, 1013.
Heinemann, U., & Saenger, W. (1982) *Nature 299*, 27.
Hendrickson, W. A., & Konnert, J. H. (1980) in *Computing in Crystallography* (Diamond, R., Ramaseshan, S., & Venkatesan, K., Eds.) pp 13.01−13.23, Indian Academy of Science, International Union of Crystallography, Bangalore, India.
Heydenreich, A., Koellner, G., Choe, H., Cordes, F., Kisker, C., Schindelin, H., Adamiak, R., Hahn, U., & Saenger, W. (1993) *Eur. J. Biochem. 218*, 1005.
Higashi, T. (1989) *J. Appl. Crystallogr. 22*, 9.
Inagaki, F., Kawano, Y., Shimada, I., Takahashi, K., & Miyazawa, T. (1981) *J. Biochem. (Tokyo) 89*, 1185.
Koepke, J., Maslowska, M., Heinemann, U., & Saenger, W. (1989) *J. Mol. Biol. 206*, 475.
Kojima, M., Mizukoshi, T., Miyano, H., Suzuki, E., Tanokura, M., & Takahashi, K. (1994) *FEBS Lett. 351*, 389.
Kostrewa, D., Choe, H., Heinemann, U., & Saenger, W. (1989) *Biochemistry 28*, 7592.
Lenz, A., Heinemann, U., Maslowska, M., & Saenger, W. (1991) *Acta Crystallogr. B47*, 521.
Lenz, A., Choe, H., Granzin, J., Heinemann, U., & Saenger, W. (1993) *Eur. J. Biochem. 211*, 311.
Martinez-Oyanedel, J., Choe, H., Heinemann, U., & Saenger, W. (1991) *J. Mol. Biol. 222*, 335.
Matthews, B. W. (1968) *J. Mol. Biol. 33*, 491.
Nishikawa, S., Morioka, H., Kim, H. J., Fuchimura, K., Tanaka, T., Uesugi, S., Hakoshima, T., Tomita, K., Ohtsuka, E., & Ikehara, M. (1987) *Biochemistry 26*, 8620.
Pletinckx, J., Steyaert, J., Zegers, I., Choe, H., Heinemann, U., & Wyns, L. (1994) *Biochemistry 33*, 1654.
Ramachandran, G. N., Ramakrishnan, C., & Sasisekharan, V. (1963) *J. Mol. Biol. 7*, 95.
Sakabe, N. (1991) *Nucl. Instrum. Methods. Phys. Res. Sect. A 303*, 448.
Sato, K., & Egami, F. (1957) *J. Biochem. (Tokyo) 44*, 753.
Shirley, B. A., Stanssens, P., Hahn, U., & Pace, C. N. (1992) *Biochemistry 31*, 725.
Steyaert, J., Hallenga, K., Wyns, L., & Stanssens, P. (1990) *Biochemistry 29*, 9064.
Sugio, S., Amisaki, T., Ohishi, H., & Tomita, K. (1988) *J. Biochem. (Tokyo) 103*, 354.
Takahashi, K. (1965) *J. Biol. Chem. 240*, 4117.
Takahashi, K. (1970a) *J. Biochem. (Tokyo) 67*, 833.
Takahashi, K. (1970b) *J. Biochem. (Tokyo) 68*, 517.
Takahashi, K. (1972) *J. Biochem. (Tokyo) 72*, 1469.
Takahashi, K., & Moore, S. (1982) *The Enzymes* XV, p 435, Academic Press Inc., New York.
Takahashi, K., Stein, W. H., & Moore, S. (1967) *J. Biol. Chem. 242*, 4682.
Walz, F. G., Jr. (1977) *Biochemistry 16*, 5509.

BI960493D